Electronic Supplementary Material (ESI) for Journal of Materials Chemistry C.

Supporting Information

Increased Crystallite Size in Thin Films of C_{60} and *p*-Terphenyls via PDMS-Assisted Crystallization

Vesta V. Zhelyaskova, Prachi Sharma, Paul I. Dron, Vikina Martinez, Josef Michl, Michael F. Toney, Daniel S. Dessau, Sean E. Shaheen*

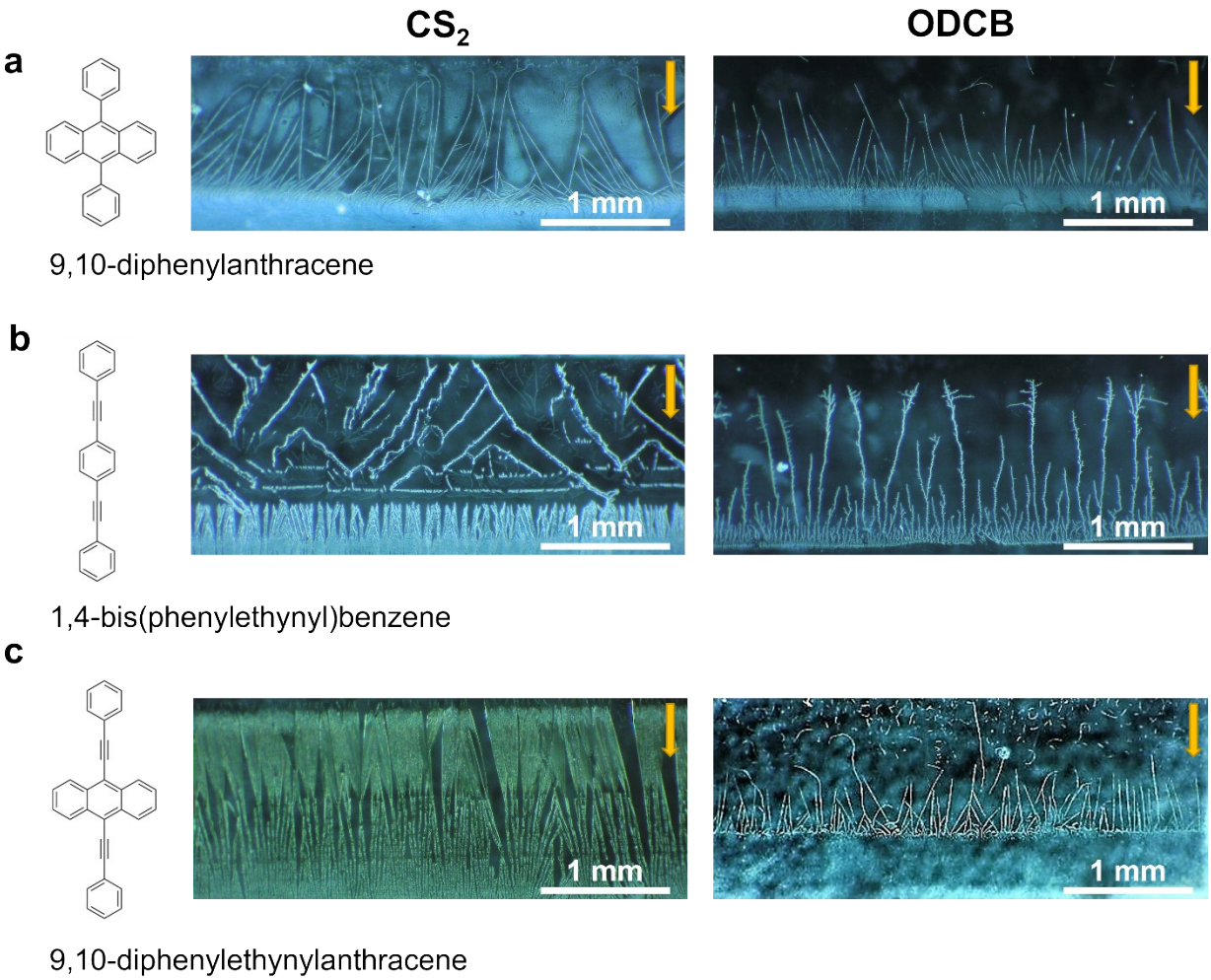

Figure S1. Optical images of three thin films of *p*-terphenyl analogues grown out of CS_2 (left column) and ODCB (right column). Film growth proceeded from the top to the bottom of the image as indicated by the yellow arrows in the images. In the case of analogues (a) and (c), the CS_2 induced much denser and larger needle-like crystallites similar to the induced growth in the C_{60} films. Analogues with naphthalene cores were unable to crystallize out of either solvent.

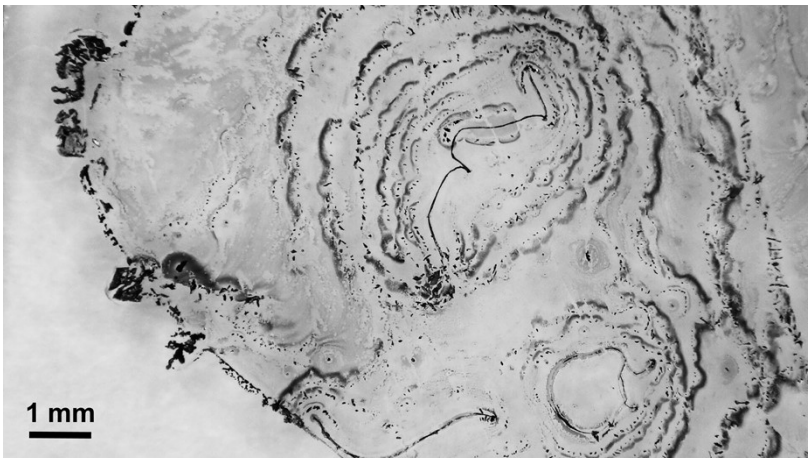

Figure S2. Optical image of thin film from drop cast solution of C_{60} in ODCB on a SAM-treated glass slide. The 50 µL of drop cast solution took 1 hour and 45 minutes to form a disordered thin film, while 50 µL of solution using the PAC method took 45 minutes to form a more ordered film with clear anisotropy. It is not apparent if the degree of crystallinity extends beyond the nanoscale.

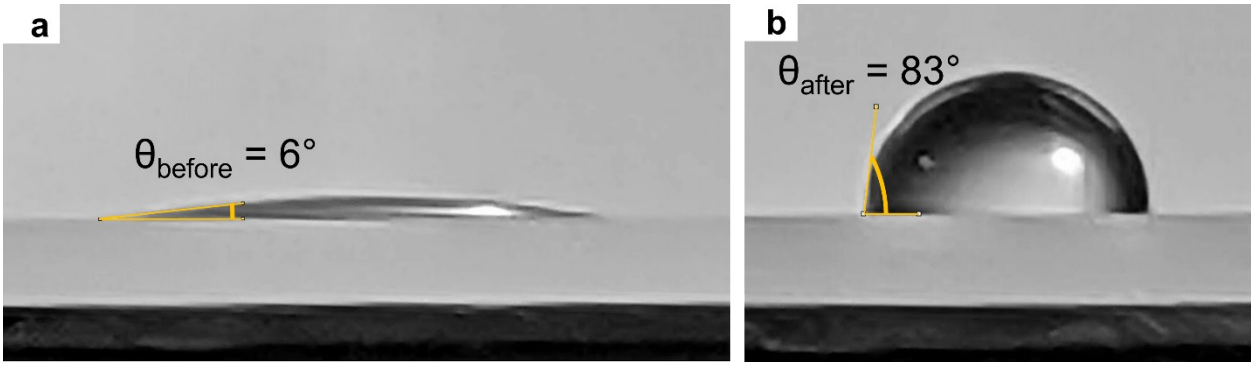

Figure S3. Optical images with contact angle measurements of DI water on (a) glass slide without SAM treatment and (b) glass slide with SAM treatment. Untreated glass slide was sonicated in cleaning solvents then cleaned in an oxygen-plasma chamber to hydroxylate the surface. The treated glass slide had the same cleaning procedure and was then left in 5 mM octadecyltrichlorosilane (OTS) toluene solution for 1 hour in ambient. Assuming a maximum contact angle of θ = 114° on OTS-treated bare silica and using Cassie's law, we estimate that after 1 hour of SAM solution treatment the coverage is ~ 70%.[S1]

[S1] Y. Yi, H. Robinson, S. Knappe, J. Maclennan, C. Jones, C. Zhu, N. Clark, J. Kitching, *J. Appl. Phys.* **2008**, 104

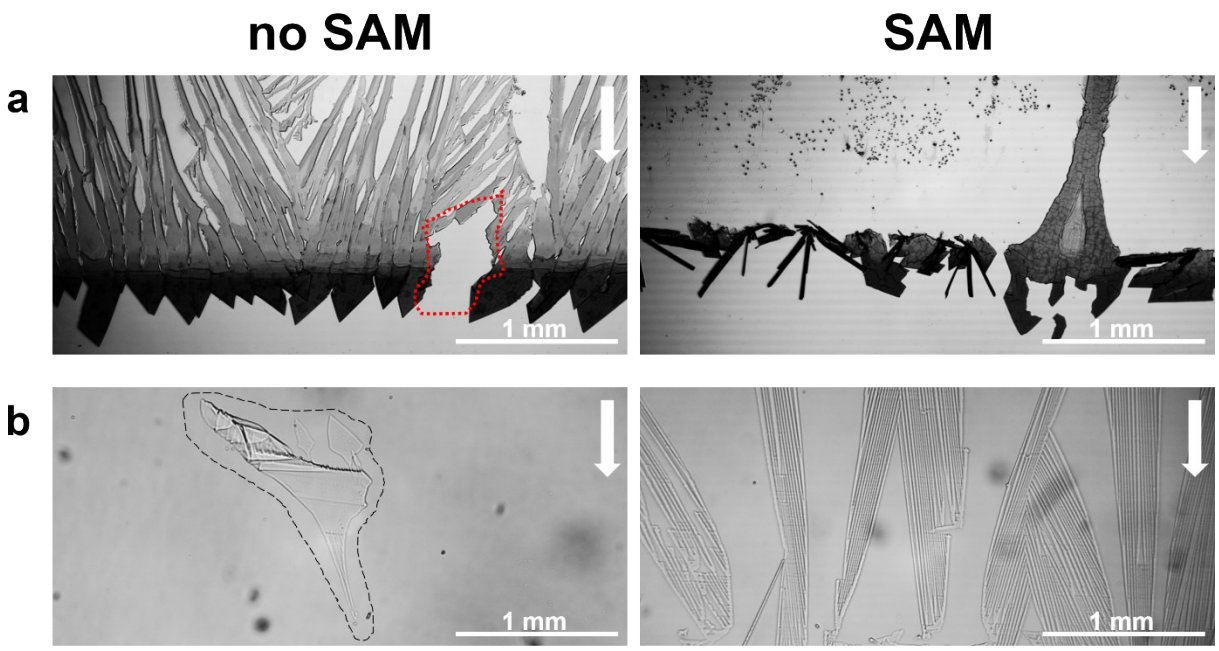

Figure S4. Contrast-enhanced optical images of (a) C_{60} / ODCB and (b) *p*-terphenyl / CS_2 crystalline thin films grown on substrates without (left) and with (right) an OTS SAM pretreatment. The crystallite in (b) grown on an untreated substrate has been outlined for clarity. This experiment highlights the unique molecule-solvent-substrate interactions that dictate the thin film growth. Although difficult to identify in these images, in both materials the SAM helped increase the adhesion of the film to the substrate. This was primarily observed by the amount of material that was lifted off the substrate with the removal of the PDMS slab and by holes left in the films like the one indicated in the left image of (a). The direction of film growth is from top to bottom of the images as indicated by the white arrows.

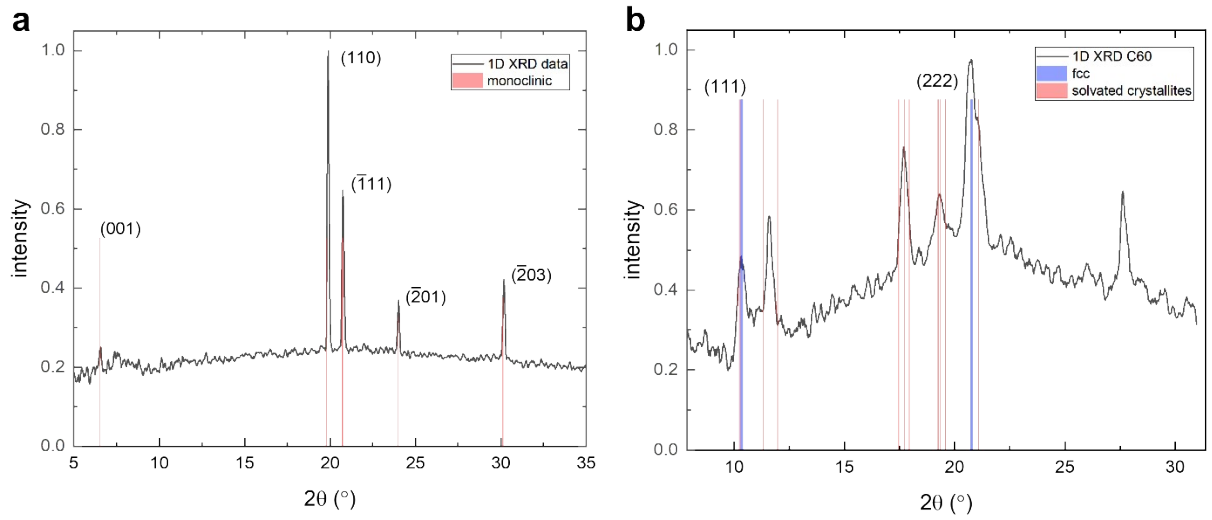

Figure S5. 1D XRD patterns from azimuthal integration of 2D GIWAXS images of (a) *p*-terphenyl and (b) C_{60} crystalline thin films grown out of CS_2. All data has been background subtracted and normalized. The calculated peak positions are overlaid on the data with the indexed peaks labeled. The indexing of the partially solvated C_{60} crystallites was beyond the scope of this paper and the calculated potential peaks of solvated orthorhombic and hcp crystal lattices are shown in red.

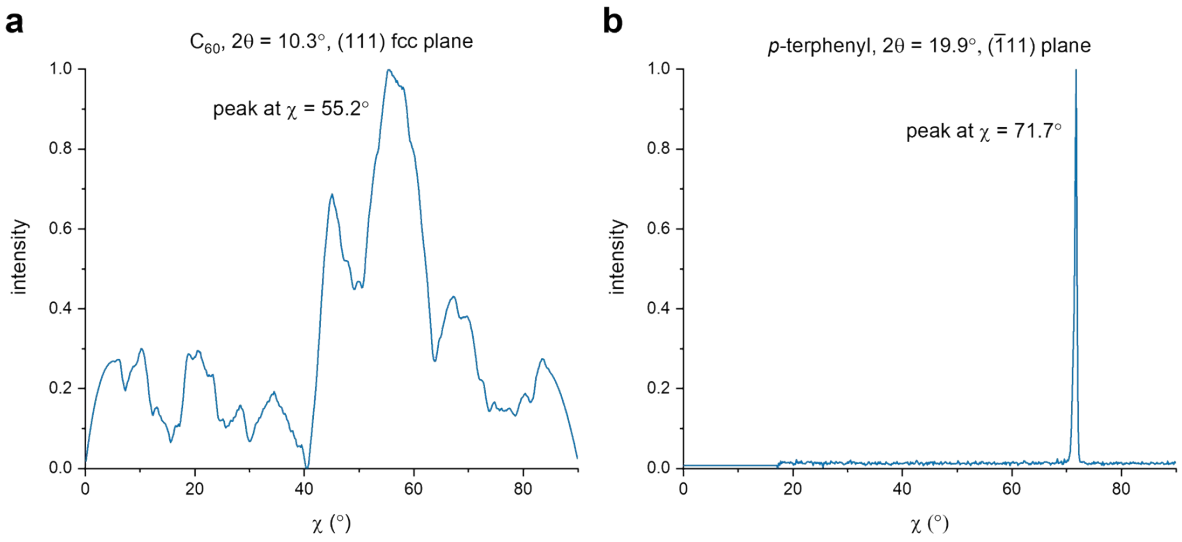

Figure S6. χ–pole plot of (a) the C_{60}/CS_2 film's (111) fcc plane and (b) the *p*-terphenyl/CS_2 film's $(11\bar{1})$. In the C_{60} film, if the (001) plane of the crystallites in the film is parallel to the substrate surface, the (111) plane would be at 54°. The broad peak centered at χ = 55° implies a preference for the molecular plane to arrange parallel to the substrate plane. In the *p*-terphenyl film, the sharp peak at χ = 71.7° (predicted to be at χ = 73°) implies that the (001) plane is almost always nearly aligned parallel to the substrate plane.

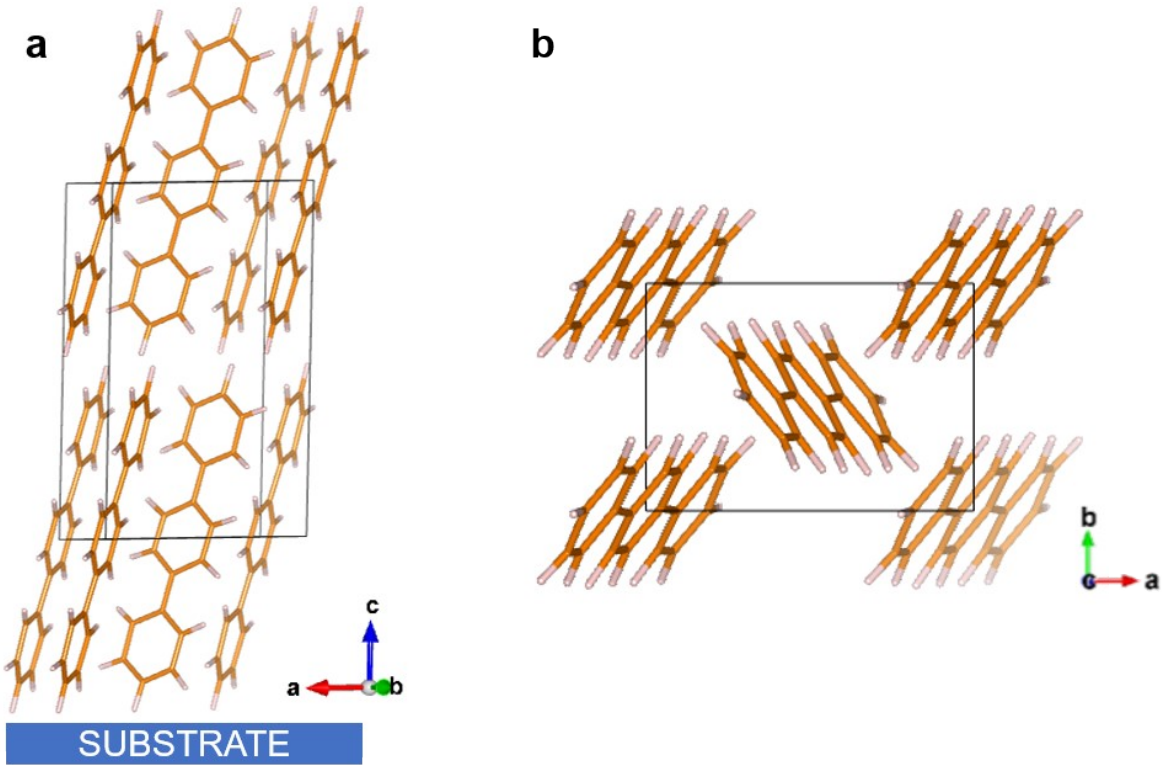

Figure S7. Orientation of *p*-terphenyl crystallites with respect to the substrate in thin films grown using the PAC method, where (a) shows a cross-sectional view and (b) shows a top-down view. Images generated using VESTA 3.[S2]

[S2] K. Momma, F. Izumi, *J. Appl. Crystallogr.* **2011**, *44*, 1272

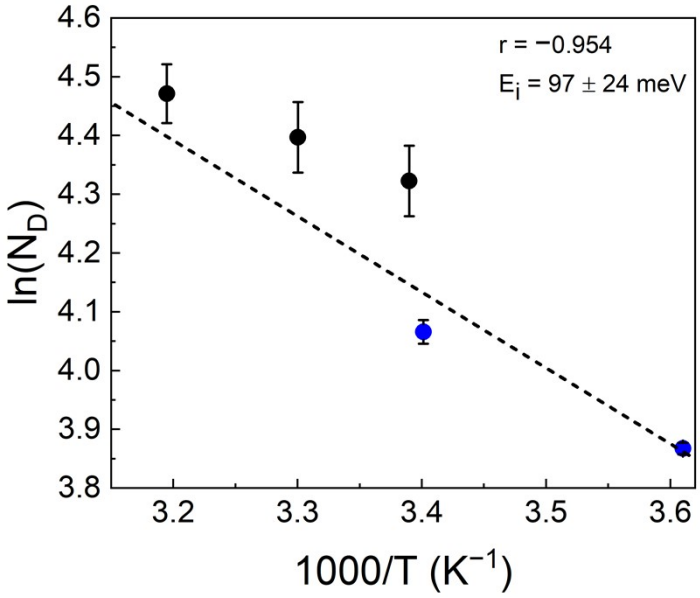

Figure S8. Arrhenius dependence of nucleation density including lower substrate temperatures (21 °C and 4 °C) of *p*-terphenyl/CS_2 PAC films grown in a different laboratory using the same experimental set up (shown in blue). The extracted energy barrier to nucleation E_i, is comparable to that extracted from data of films grown at higher substrate temperatures.

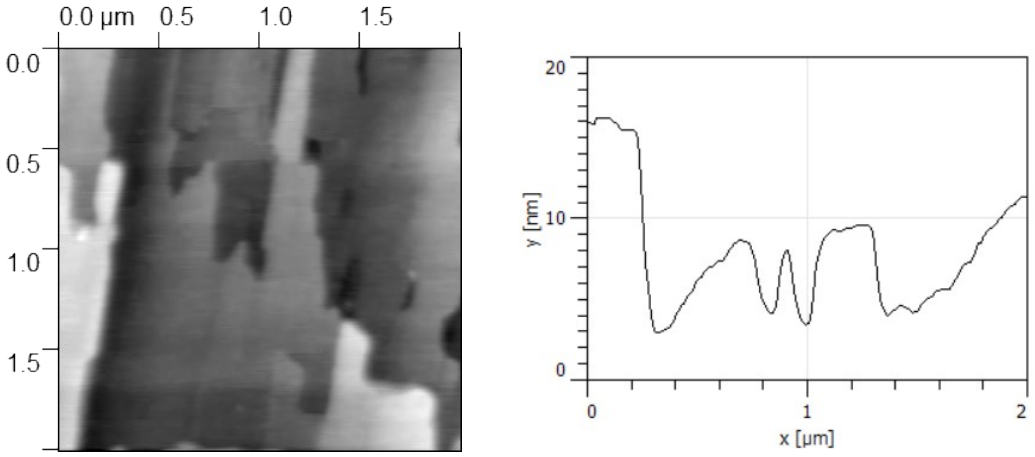

Figure S9. AFM image of C_{60} crystalline needle surface (left) and corresponding line profile (right). Although the crystalline thin film growth is initially 3D, the layering on the crystallite surface indicates 2D growth.

I. Surface Hydroxylation and SAM Pretreatment

Our experiments show that hydroxylation and SAM pretreatment of the substrates can allow for gold patterning of thin film growth using PAC. In our preliminary experiments to incorporate the solution-grown crystalline thin films into transistor geometries, films were grown as active layers onto glass substrates with evaporated gold contacts. First, the substrates were cleaned in a sonication bath with acetone, methanol, and isopropyl alcohol followed by 10 minutes in an oxygen plasma (OP) cleaner. Gold contacts were evaporated onto the substrates immediately following the OP cleaning. Some substrates were then directly put into an OTS solution for the SAM pretreatment, others had thin films grown on them immediately.

On the substrates with evaporated gold contacts and without the SAM pretreatment, the tendrils of the C_{60}/ODCB films preferentially nucleated and grew along the contacts. During the formation of the thin film, the molecules preferentially nucleated on the rough, recently evaporated gold surface while avoiding the uncovered, activated glass surface. However, on the substrates with the SAM pretreatment, the film growth showed no preference for the nucleation on the gold. The OTS monolayer seemed to evenly bond to both the exposed glass and evaporated gold during its formation. Optical images reveal no difference between the average nucleation density on the gold and that on the glass (Fig. S10a), while in the optical images of the sample without the SAM pretreatment the difference in nucleation density between the two areas on the substrate is stark (Fig S10b).

Omitting the SAM pretreatment on gold patterned substrates, while potentially sacrificing crystallite size and quality, can help pattern the thin films deposited on the substrates. This controlled patterning of crystalline organic thin film growth via substrate pretreatment variation could prove beneficial in the industrial development of organic electronic devices.

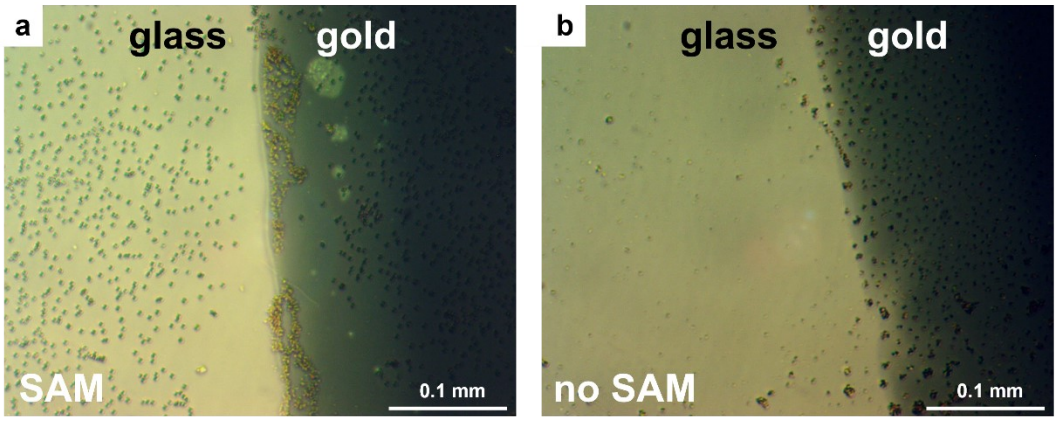

Figure S10. Optical images of a glass substrate with an early stage of PAC C_{60} thin film growth (a) with and (b) without OTS SAM pretreatment. The images show the varying nucleation density on the gold versus glass with different substrate pretreatments. (c) Optical image of preferential growth of large crystallites on the evaporated gold without the SAM pretreatment.

II. Nucleation Density Analysis and Arrhenius Fit

The surface and linear nucleation density (N_D) for C_{60}/ODCB and *p*-terphenyl/CS_2 respectively was determined using ImageJ. For each sample, the average number of nucleation sites per pixel was calculated along the same region in the film growth as indicated in Fig. S11. Maintaining the counting along the same position laterally, we can assume that the solution was at the same concentration and the film was at the same stage in its growth across the sample. We note that the nucleation sites in the ODCB-grown films are likely the result of dewetting processes at play. However, even if the formation of these islands is governed by solution dewetting, the islands can still be used as a proxy for nucleation sites because they likely contain at least one crystalline nuclei.[S3]

For the C_{60} film surface N_D calculation, nucleated islands per some arbitrarily sized square were counted, averaged, and converted to islands per mm^2. For the *p*-terphenyl film linear N_D calculation, the number of nucleated needles per set of needles was counted and converted to nucleated needles per mm. Sections of the *p*-terphenyl growth from which the needle linear density is determined are chosen at the transition from diverging to parallel growth. Each film shows diverging, "umbrella" nucleation sections which end in long parallel needles. Near the top of these sections, the needles are not yet parallel or are often interrupted by excess deposited material. By the edge of the film, the growth is entirely uninterrupted, parallel needles. Because we need to determine nucleation density, which is occurs early in the film growth, we needed to quantify the growth somewhere at the top of the film growth. We chose to quantify the needles starting as close to this transition from "umbrella-ed" to parallel needles as we could.

The determined N_D values were then fitted to the Arrhenius equation (Equation 1) at the different substrate temperatures to determine our experiment-specific crystal formation energy, E_i.

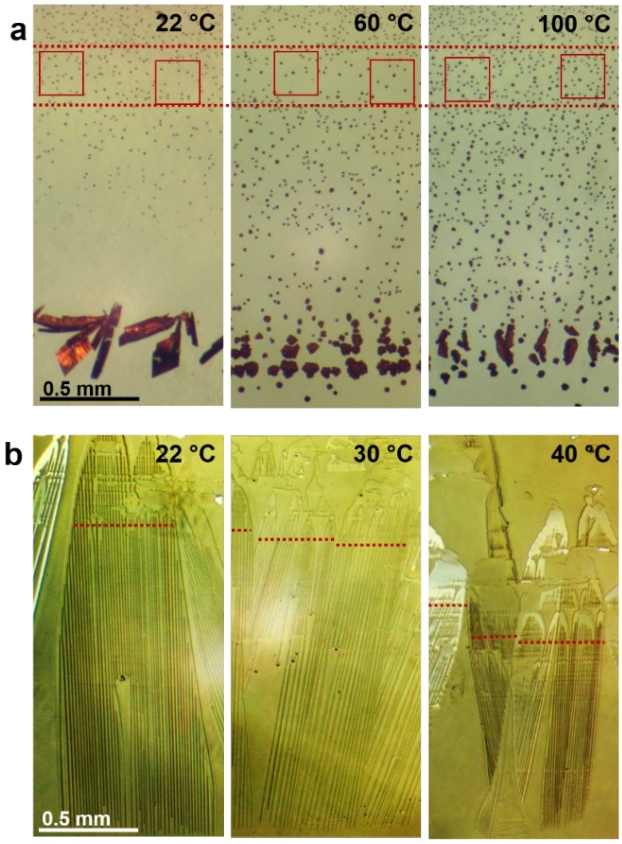

Figure S11. (a) POM images of C_{60}/ODCB thin films grown at different T_S with region of thin film growth used to determine N_D and E_i bounded by the dashed lines and examples of the arbitrary squares used to calculate the average density per mm^2. (b) Contrast-enhanced POM images of *p*-terphenyl/CS_2 thin films grown at different T_S with examples of the sets of needles counted across the dashed lines to determine the linear N_D for the E_i calculation. The location of the dashed lines was chosen to be at the transition between diverging and parallel crystallites, determined through visual inspection of magnified images.

[S3] J.-N. Tisserant, G. Wicht, O. Gobel, E. Bocek, G.-L. Bona, T. Geiger, R. Hany, R. Mezzenga, S. Partel, P. Schmid, W. B. Schweizer, J. Heier, *ACS Nano*, **2013**, 7, 6

solvent	% change in PDMS mass	relative polarity [S4]
Methanol	+0.13	0.762
Ethanol	+1.96	0.654
Acetonitrile	+0.08	0.460
Acetone	+2.41	0.355
ODCB	+7.21	0.225
CS_2	+11.40	0.065

Table S1. Experiments in PDMS solvent uptake. Pieces of PDMS immersed in solvents ranging from polar to nonpolar (arranged top to bottom in table) for a set time were massed before and immediately after the solvent exposure. The percent change in mass was found to negatively correlate with relative polarity.

[S4] C. Reichardt, *Solvents and Solvent Effects in Organic Chemistry*, Wiley-VCH Publishers, 3rd ed., **2003**, Appendix, 471-507